

# Suppression of chlorine activation on aviation-produced volatile particles

S. K. Meilinger<sup>1</sup>, B. Kärcher<sup>2</sup>, and Th. Peter<sup>3</sup>

<sup>1</sup>MPI für Chemie, Mainz, Germany

<sup>2</sup>DLR Oberpfaffenhofen, Institut für Physik der Atmosphäre, Wessling, Germany

<sup>3</sup>ETH Laboratorium für Atmosphärenphysik, Zürich, Switzerland

Received: 15 May 2002 – Published in Atmos. Chem. Phys. Discuss.: 15 July 2002

Revised: 15 October 2002 – Accepted: 21 October 2002 – Published: 5 November 2002

**Abstract.** We examine the effect of nanometer-sized aircraft-induced aqueous sulfuric acid ( $\text{H}_2\text{SO}_4/\text{H}_2\text{O}$ ) particles on atmospheric ozone as a function of temperature. Our calculations are based on a previously derived parameterization for the regional-scale perturbations of the sulfate surface area density due to air traffic in the North Atlantic Flight Corridor (NAFC) and a chemical box model. We confirm large scale model results that at temperatures  $T > 210$  K additional ozone loss – mainly caused by hydrolysis of  $\text{BrONO}_2$  and  $\text{N}_2\text{O}_5$  – scales in proportion with the aviation-produced increase of the background aerosol surface area. However, at lower temperatures ( $< 210$  K) we isolate two effects which efficiently reduce the aircraft-induced perturbation: (1) background particles growth due to  $\text{H}_2\text{O}$  and  $\text{HNO}_3$  uptake enhance scavenging losses of aviation-produced liquid particles and (2) the Kelvin effect efficiently limits chlorine activation on the small aircraft-induced droplets by reducing the solubility of chemically reacting species. These two effects lead to a substantial reduction of heterogeneous chemistry on aircraft-induced volatile aerosols under cold conditions. In contrast we find contrail ice particles to be potentially important for heterogeneous chlorine activation and reductions in ozone levels. These features have not been taken into consideration in previous global studies of the atmospheric impact of aviation. Therefore, to parameterize them in global chemistry and transport models, we propose the following parameterisation: scale the hydrolysis reactions by the aircraft-induced surface area increase, and neglect heterogeneous chlorine reactions on liquid plume particles but not on ice contrails and aircraft induced ice clouds.

Correspondence to: S. K. Meilinger  
(smeili@mpch-mainz.mpg.de)

## 1 Introduction

In view of the present and anticipated growth rates of commercial aviation, there is increasing concern about the environmental impact of the associated emissions on atmospheric ozone ( $\text{O}_3$ ) chemistry. While recent assessments concentrated on the response of  $\text{O}_3$  to gaseous nitrogen compounds ( $\text{NO}_x$ ) and water vapor ( $\text{H}_2\text{O}$ ) emissions (WMO, 1994; Brasseur et al., 1998), aerosols and contrails formed in aircraft exhaust plumes may also play an important role (IPCC, 1999; Kawa et al., 1999). Such particles can significantly enhance the aerosol surface area available for heterogeneous reactions (Hofmann et al., 1998; Anderson et al., 1999). Global model calculations suggest the additional heterogeneous chemistry in the perturbed aerosol layer to have a net  $\text{O}_3$  depleting effect, with the highest values predicted north of the NAFC (Weisenstein et al., 1998; Pitari et al., 2001). These calculations (Weisenstein et al., 1998) indicate that the ozone depleting effect of aircraft particle emissions depends on temperature ( $T$ ) and on the size and number densities of the emitted particles at plume breakup (time  $\tau$  after which the plume can be considered a regional scale perturbation). However, these simulations did not account for the temperature feedback on particle number densities at plume breakup nor the different chemical reactivity of the nm-sized aircraft particles, compared to the background aerosols of typical size 100 nm, due to the Kelvin effect (exponential decrease of solubility due to surface curvature following  $\exp[-\text{const.}/r]$ , where  $r$  is the particle radius).

In general, the rate of a given heterogeneous reaction,  $k \propto \gamma A$ , is determined by the reactive uptake coefficient  $\gamma$  and the aerosol surface area density  $A$  (in units of  $\text{cm}^2\text{cm}^{-3}$ ), both of which depend on  $T$ . While the  $T$ -dependence of  $A$

is independent of the chemical reaction under consideration, that of  $\gamma$  ranges from weak for concentration-independent reactions (e.g. hydrolyses of  $\text{N}_2\text{O}_5$  or  $\text{BrONO}_2$ ) to pronounced for reactions depending on the reactant solubilities, e.g. for  $\text{ClONO}_2 + \text{HCl}$  (Hanson et al., 1994). Due to the Kelvin effect, the reactive uptake of chemical compounds by aircraft particles (subscript  $a$ ) might be limited in comparison to background particles (subscript  $b$ ), i.e.  $\gamma_a < \gamma_b$ . Furthermore, the Kelvin effect limits the solubility of  $\text{H}_2\text{O}$  and  $\text{HNO}_3$  and thus the growth of the small aircraft particles compared to the larger background aerosols ( $|dA_a/dT| < |dA_b/dT|$ ). In addition, the particle size dependence of coagulation scavenging leads to increasing scavenging losses of aircraft particles as background aerosols grow more readily in cooling air masses. This may significantly reduce the aircraft-induced surface area at plume breakup,  $A_a(\tau)$ , leading to  $A_a(\tau) \ll A_b$  at low temperatures. Therefore reliable estimates for liquid surface area perturbations due to air traffic are required that can account for such dependences. Introducing the concept of an “average plume decay time” as a criterion for plume breakup, we have previously derived such estimates of size spectrum and surface area perturbation of the volatile plume particles as a function of air traffic density and background aerosol surface area density (Kärcher and Meilinger, 1998) among other parameters, and employ these results in the present study. Using a stationary photochemical box model (Groß, 1996; Meilinger et al., 2001), we examine heterogeneous ozone chemistry on aircraft-produced particles as a function of temperature including the Kelvin effect and coagulation processes between aircraft-induced  $\text{H}_2\text{SO}_4/\text{H}_2\text{O}$  and background particles. Our results apply best to the stratospheric part of the NAFC, where relatively long particle residence times (days to weeks) cause surface area perturbations from subsonic aircraft to be largest (IPCC, 1999, , Chapter 3, pp. 65-120). We will show that at cold lowermost stratospheric conditions enhanced scavenging and Kelvin effect render heterogeneous chlorine chemistry on nm-sized aircraft particles largely inefficient. Further, our results allow for a simple parameterization scheme for heterogeneous hydrolysis and halogen chemistry on aviation-produced liquid aerosols suited for implementation in global models.

## 2 Model description

We employ an extended version (Meilinger et al., 2001) of the Mainz Photochemical Box Model (see Groß, 1996, for details). Net ozone production rates,  $P(\text{O}_3)$ , are averaged over 24 hours to account for the diurnal cycle, assuming constant latitude ( $50^\circ\text{N}$ ) and applying the  $\text{O}_3$  profile of the U.S. standard atmosphere. The model includes complete diurnal chemistry for  $\text{NO}_y$ ,  $\text{Cl}_y$ ,  $\text{Br}_y$ ,  $\text{HO}_x$ ,  $\text{O}_x$ , methane, ethane, acetone and their oxidation products. For gas phase reactions, we used the kinetic reaction rates recommended by Atkinson

et al. (1999) and DeMore et al. (1997) considering the update by Sander et al. (2000). Photolysis rates were calculated with an update (Becker et al., 2000) of the scheme by Lary and Pyle (1991).

More importantly, the model includes heterogeneous reactions of  $\text{N}_2\text{O}_5$ , bromine and chlorine species on liquid and ice particles. For heterogeneous halogen and  $\text{N}_2\text{O}_5$  chemistry we assumed the uptake coefficients evaluated for polar stratospheric clouds (Sander et al., 2000) to be applicable to tropopause conditions. The liquid particles are assumed to be composed of aqueous  $\text{H}_2\text{SO}_4$ , which may take up  $\text{H}_2\text{O}$ ,  $\text{HNO}_3$ ,  $\text{HCl}$ ,  $\text{HOCl}$ ,  $\text{HBr}$  and  $\text{HOBr}$  at sufficiently low temperatures. The new model version accounts for heterogeneous processes on background as well as on aviation-produced aerosols. In the evaluation of heterogeneous reaction rates, we distinguish reactive uptake coefficients and available surface area densities of both particle types.

While background aerosol surface area density is calculated according to Carslaw et al. (1995), the size distribution and surface area density of the aircraft-induced liquid particles are calculated according to the parameterization of Kärcher and Meilinger (1998). Their estimates account for a variety of parameters controlling the aircraft aerosol at the average plume decay time: the conversion of fuel sulfur into ultrafine sulfate particles ( $\eta = 5\%$ ), the plume mixing with ambient air, and the background aerosol surface area, which – due to uptake of  $\text{HNO}_3$  – is  $T$ -dependent.

Uptake coefficients,  $\gamma_{ij}^{eff}$ , for heterogeneous reactions of molecules  $i$  adsorbed on the surface and reacting with molecules of species  $j$  are calculated according to  $1/\gamma_{ij}^{eff}(r) = 1/\alpha_i + 1/\gamma_{ij}^{react} + 4Kn/3$ , where the first term describes pure physisorption (with the mass accommodation coefficient  $\alpha_i$ ),  $\gamma_{ij}^{react}$  is the reaction probability of the adsorbed molecules, and the last term describes the case when vapor transport to the particle surface is limited by gas phase diffusion (with the Knudsen number  $Kn$ , only important for large particles, i.e. in the case of ice particle formation). While constant  $\gamma_{ij}^{react}$  is assumed for heterogeneous reactions on ice, for liquid phase reactions  $\gamma_{ij}^{react}$  generally depends on the reactants solubilities  $H_{ij}$  (Hanson et al., 1994; Peter, 1997). Due to the Kelvin barrier, the solubilities depend exponentially on particle radius ( $H_{ij}(r) \propto \exp[-r_{cr}/r]$ ). This exponential dependence strongly limits the uptake coefficient  $\gamma_{ij}$  for particles smaller than or about equal to the critical radius  $r_{cr} = 2\sigma v_{i,j}/(RT)$ . Using the typical values  $\sigma = 0.08 \text{ J/m}^2$ ,  $v_{\text{HCl}} = 28.56 \text{ cm}^3/\text{mol}$ ,  $T = 200 \text{ K}$ , and  $R = 8.314 \text{ JK}^{-1}\text{mol}^{-1}$  yields  $r_{cr} \simeq 2 \text{ nm}$ , which is comparable to the mean radius of aviation-produced liquid particles (Kärcher et al., 2000). We averaged  $\gamma_{ij}$  over the respective size distribution of liquid aerosol particles to account for the fraction of larger particles which dominate the effective uptake.

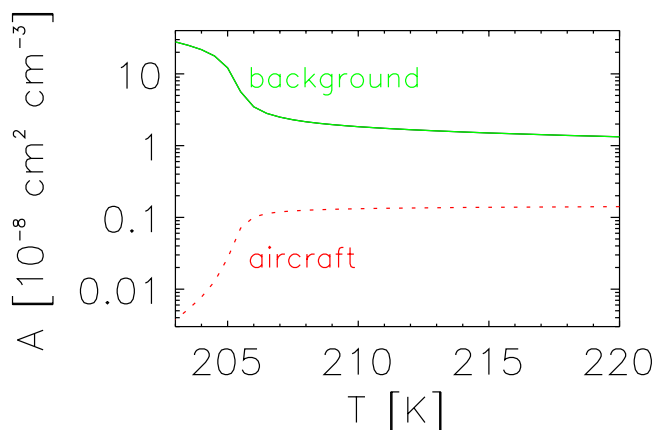


**Fig. 1.** Surface area densities [ $\mu\text{m}^2\text{cm}^{-3}$ ] of background (green solid curve) and aircraft-generated (red dotted curve)  $\text{H}_2\text{SO}_4/\text{H}_2\text{O}$  particles in the NAFC as a function of temperature, the latter calculated according to the method of Kärcher and Meilinger (1998) using temperature-dependent background aerosol surface areas (Carslaw et al., 1995) assuming 25 ppmv  $\text{H}_2\text{O}$ , 0.87 ppbv  $\text{HNO}_3$  and a background number density of  $50 \text{ cm}^{-3}$  containing 100 pptv  $\text{H}_2\text{SO}_4$ .

### 3 Effects of aviation-produced aerosols on ozone

#### 3.1 Particle scavenging

Depending on the variability of the background aerosol surface area density,  $A_b$ , typical ranges of the relative surface area perturbation at the average plume decay time,  $A_a(\tau)/A_b$ , in the NAFC are 0.03 – 20% for the present subsonic air traffic in the tropopause region (Kärcher and Meilinger, 1998). The magnitude of this perturbation is mainly determined by the surface area density of the background aerosols which scavenge the smaller aircraft particles. The above range of perturbations has been determined for average temperatures at the tropopause and does not include very cold cases, in which the associated variability could be larger, as shown below. The coagulation efficiency becomes strongly enhanced when the background particles grow due to condensation of  $\text{H}_2\text{O}$  and  $\text{HNO}_3$  at temperatures below the  $\text{HNO}_3$  dew point,  $T_d$  (the temperature at which the liquid  $\text{HNO}_3$  mass fraction becomes equal to that of  $\text{H}_2\text{SO}_4$ ).

Figure 1 shows  $A_a(\tau)$  and  $A_b$  as a function of  $T$  starting with  $A_a(\tau)/A_b = 10\%$  at  $T = 220 \text{ K}$ , which is the value after an average plume decay time of 1 – 2 days, representative for the traffic density in the NAFC (we use 45.8 h in this study, following Kärcher and Meilinger, 1998). Note that without scavenging by the background aerosols (i.e. allowing only for self-coagulation and dilution of the aircraft aerosols) there would be about 30% more aircraft-derived liquid particles (at 220 K).

At temperatures above  $T_d$  (here 205.5 K), surface area

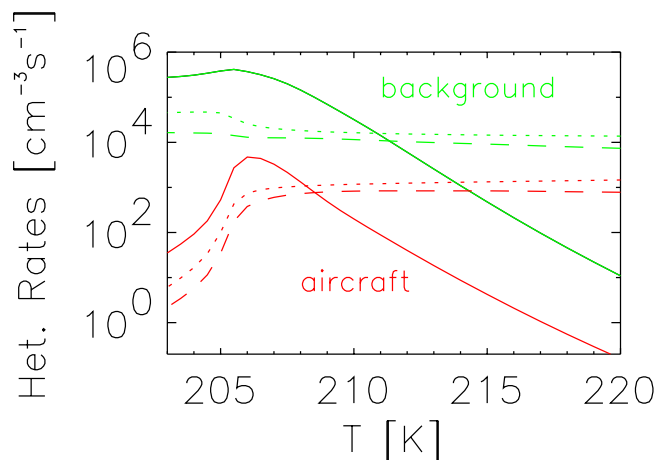


**Fig. 2.** Heterogeneous reaction rates of  $\text{ClONO}_2+\text{HCl}$  (solid curves),  $\text{N}_2\text{O}_5+\text{H}_2\text{O}$  (dotted) and  $\text{BrONO}_2+\text{H}_2\text{O}$  (dashed curves) due to background aerosol (green curves) and due to particles from aircraft (red curves). Same conditions as in Fig. 1, assuming typical lowermost stratospheric concentrations (Hendricks et al., 1999) with 325 pptv  $\text{Cl}_y$ , 2.78 pptv  $\text{Br}_y$ , 275 ppbv  $\text{O}_3$ , 44 ppbv  $\text{CO}$ , and 1.7 ppmv  $\text{CH}_4$ . Typical  $\text{NO}_x$  mixing ratios of 0.2 ppbv for the NAFC were taken from Ziereis et al. (2000). NMHC levels of 100 pptv  $\text{C}_2\text{H}_6$  and 100 pptv acetone were taken from Singh et al. (1997).

densities of background and aircraft aerosols vary only weakly (Fig. 1). However, below  $T_d$  the background particles take up  $\text{H}_2\text{O}$  and a substantial fraction of the total  $\text{HNO}_3$  (34% at 205 K), yielding larger particles. Consequently, coagulation rates increase and the surface area density of the aviation-produced particles decreases by more than an order of magnitude at 200 K.

#### 3.2 Kelvin effect

Figure 2 shows the dominant heterogeneous reaction rates  $k_a$  and  $k_b$  for aircraft (red) and background (green) particles, respectively. It illustrates the leading role of the hydrolysis of  $\text{BrONO}_2$  (dashed) and  $\text{N}_2\text{O}_5$  (dotted) at high and moderate temperatures. These reactions are assumed to be independent of the reactant solubilities, but depend mainly on surface area densities. Consequently, there is little dependence on  $T$  above  $T_d$ , and  $k_a/k_b \simeq 10\%$ , which is in agreement with the surface area ratio. The decrease in  $k_a$  below  $T_d$  corresponds to the reduction in  $A_a$  due to enhanced scavenging (Fig. 1), while the increase of  $k_b$  is mainly caused by growth of  $A_b$  (but reduced due to the consumption of the reactants).

As temperatures approach  $T_d$ , however, solubility-dependent chlorine activation gains importance and  $\text{ClONO}_2+\text{HCl}$  (solid curves) becomes the most important reaction path. However, due to the Kelvin effect, the solubility of  $\text{HCl}$  in aviation-induced aerosols remains low, and hence  $k_a/k_b < A_a(\tau)/A_b$ .

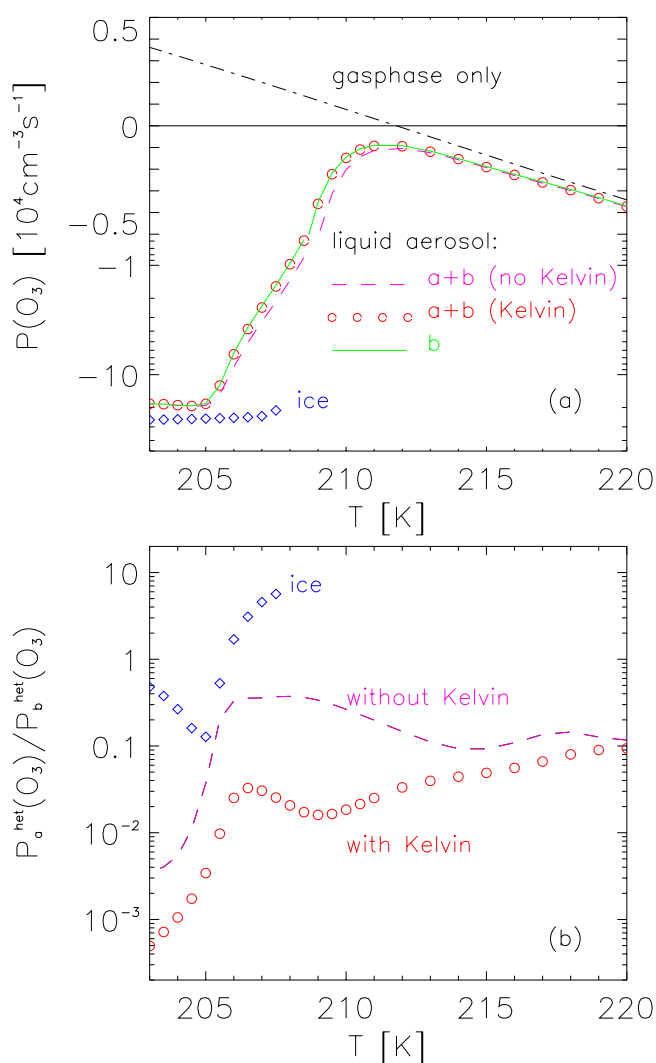


**Fig. 3.** (a) Averaged net ozone production rates  $P(\text{O}_3)$  at 200 hPa and  $50^\circ\text{N}$  as a function of temperature assuming no aerosol (black dash-dotted curve),  $50 \text{ cm}^{-3}$  background aerosol particles containing 100 pptv  $\text{H}_2\text{SO}_4$  (green solid curve), background aerosol mixed with aviation-induced aqueous  $\text{H}_2\text{SO}_4$  particles in the North Atlantic flight corridor with (red circles) and without (violet dashed curve) Kelvin effect, and  $4.2 \text{ cm}^{-3}$  ice particles from an aged contrail or cirrus (blue diamonds). (b) Heterogeneous ozone production rates relative to background aerosol (green solid curve in (a)). Symbols as in Fig. 2 showing the relative effect of liquid aircraft particles with (red circles) and without (violet dashed curve) Kelvin effect, and for ice particles (blue diamonds). Same conditions as Figs. 1 and 2.

### 3.3 Ozone destruction on liquid aircraft particles

Figure 3 summarizes these results in terms of net effects on ozone. The black dash-dotted curve in Fig. 3a shows the net ozone production rates  $P(\text{O}_3)$  for gas phase chemistry only. The green solid curve additionally considers heterogeneous chemistry on the background aerosol (Meilinger et al., 2001).

The violet dashed curve and the red circles additionally include the liquid aircraft aerosols, with (red circles) and without (violet dashed curve) the Kelvin effect, while the blue diamonds show the effect after including contrail ice particles assuming number densities and surface areas which correspond to the same degree of entrainment that was assumed for the non-contrail plume. At temperatures above  $\sim 214 \text{ K}$  (corresponding roughly to the zonal mean value at 200 hPa and  $50^\circ\text{N}$ ), heterogeneous chemistry increases gas phase  $\text{O}_3$  destruction by  $\sim 500 \text{ cm}^{-3} \text{ s}^{-1}$ . At low temperatures ( $T < 210 \text{ K}$ )  $P(\text{O}_3)$  takes on large negative values, which are up to a factor of 20 larger than the gas phase-driven production. This is due to heterogeneous activation of chlorine caused by the enhanced solubility of  $\text{HCl}$  in the liquid background aerosol particles which grow as  $T$  approaches  $T_d$ .

In contrast, liquid aircraft-induced particles show a completely different temperature effect on  $\text{O}_3$  loss than the background particles. Figure 3b contains the same information as Fig. 3a but expressed as the fraction of  $\text{O}_3$  change due to heterogeneous chemistry on aviation particles normalized by the heterogeneous effect of the background aerosols only, i.e.  $P_a^{\text{het}}(\text{O}_3)/P_b^{\text{het}}(\text{O}_3)$ , where  $P_b^{\text{het}}(\text{O}_3) = P_b(\text{O}_3) - P_{\text{gas}}(\text{O}_3)$  and  $P_a^{\text{het}}(\text{O}_3) = P_{a+b}(\text{O}_3) - P_b^{\text{het}}(\text{O}_3) - P_{\text{gas}}(\text{O}_3)$ .

At high  $T$ , the additional effect of aviation aerosols on  $\text{O}_3$  rates is about 10%, close to the size of the surface area perturbation  $A_a/A_b$ . Under these conditions, the Kelvin effect becomes unimportant, as the  $\text{N}_2\text{O}_5$  and  $\text{BrONO}_2$  hydrolysis reactions are independent of solubilities, but rather are surface contact-driven. At low  $T$ , however, the relative impact of  $\text{H}_2\text{SO}_4/\text{H}_2\text{O}$  particles from aircraft decreases to below 1% when neglecting the Kelvin effect, and even below 0.1% when including the Kelvin effect.

Thus both, temperature-enhanced scavenging and the Kelvin effect limit the relative effect of aviation-produced aerosol on heterogeneous chemistry under cold conditions (Fig. 3b), while  $\text{O}_3$  depletion increases by more than two orders of magnitude as  $T$  decreases from 210 to 203 K (Fig. 3a). In contrast, under warmer conditions the heterogeneous effect of aviation-produced droplets scales in proportion to the surface area perturbation.

### 3.4 Ozone destruction on contrail ice particles

In the tropopause region,  $T_d$  lies several Kelvin below the ice frost point ( $T_{\text{ice}}$ ), so that freezing and cirrus cloud formation may occur before the air becomes chemically processed by the liquid particles (Kärcher and Solomon, 1999). Persistent contrails form in ice-supersaturated air. This may pave the way for efficient regional-scale heterogeneous chemistry (Borrmann et al., 1996; Kärcher, 1997).

The blue diamonds in Fig. 3 show the effect of ice particles (originating, for example, from an aged contrail) on  $\text{O}_3$  loss below the frost point at 207.6 K (while all other curves ignore transient or persistent ice formation). Recall that we

assume the uptake coefficients involving ice surfaces according to Sander et al. (2000) in our model to be applicable to tropopause conditions. The increase of heterogeneous  $O_3$  loss is caused by chlorine activation on ice surfaces and exceeds the effect of supercooled ternary background aerosol by up to a factor of 10. At the same time, the presence of ice diminishes the effect of heterogeneous chemistry on the liquid particles (not shown) due to gas phase dehydration and accelerated scavenging.

In summary, at temperatures below the frost point, enhanced  $O_3$  loss due to additional aircraft-induced chlorine activation on contrails or contrail-cirrus is important; in comparison, chlorine activation due to liquid particles from aircraft emissions can be neglected.

#### 4 Conclusions

We have shown for temperatures  $T > 210$  K in the lowermost stratosphere, that the effect of subsonic aircraft-induced  $H_2SO_4/H_2O$  aerosols on heterogeneous ozone chemistry is dominated by the hydrolysis of  $BrONO_2$  and  $N_2O_5$ , which – because they are solubility independent – scale directly with the increase of available aerosol surface area. This highlights the importance of reliable estimates of the surface area perturbation in global model simulations.

Relative to background aerosols, the chemical effects of aircraft-emitted volatile particles on atmospheric ozone decreases with decreasing temperature (Fig. 3b). Below the dew point of  $HNO_3$ , chlorine activation caused by the new liquid particles is limited by reduced solubilities of reacting gases (Kelvin effect) and by enhanced scavenging losses due to the swelling background particles. Therefore, additional chlorine activation due to aircraft-produced volatile particles can be neglected. Below the ice frost point,  $O_3$  loss rates caused by chlorine activation in persistent contrails or contrail-induced ice clouds exceed those on supercooled droplets by as much as an order of magnitude, provided the heterogeneous reaction rates validated for stratospheric conditions can be applied to ice particles at subsonic cruising altitudes.

This suggests the following simple parameterization for the heterogeneous  $N_2O_5$  and halogen chemistry on aviation-produced particles:

- for  $T > T_{ice}$  scale  $BrONO_2$  and  $N_2O_5$  hydrolysis by  $(A_a + A_b)/A_b$  without Kelvin effect;
- for  $T < T_{ice}$  take chlorine activation on ice particles into account.

This parameterization can be easily applied in large-scale atmospheric models.

Similar calculations (UBA, 2000) reveal that these mechanisms also work under lower stratospheric conditions at the cruising altitude of supersonic aircraft (above 16 km). As a

consequence, the strong sensitivity of stratospheric  $O_3$ -losses on the size and number of aircraft-produced  $H_2SO_4/H_2O$  particles as suggested by global chemical transport models (Weissenstein et al., 1998) is likely to be removed. Simulations including our proposed parameterization scheme are needed to confirm this conjecture.

Recent assessments emphasized that for a future supersonic aircraft fleet, the impact of particle emissions may nearly double the calculated  $O_3$  loss relative to  $NO_x$  and  $H_2O$  emissions alone (Kawa et al., 1999). At moderate and high temperatures the aviation-induced surface area increase (up to about a factor of two in supersonic flight corridors; Kärcher and Meilinger, 1998) would indeed considerably affect heterogeneous chemistry. However, under cold conditions such as the winter polar stratosphere, scavenging and Kelvin effect limit the chemistry on aviation-produced liquid aerosols. On the other hand, contrails may develop into long-lived polar stratospheric clouds (likewise not yet being considered in global assessment studies), which might enhance chlorine activation (Peter et al., 1991). The overall effect should be subject to future global assessments.

*Acknowledgements.* This work was supported by the Umweltbundesamt (Berlin, Germany) under contract 104 02 814, and by the project “Particles in the Upper Troposphere and Lower Stratosphere and Their Role in the Climate System” (PARTS) funded by the European Commission.

#### References

- Anderson, B. E., Cofer, W. R., Crawford, J., Gregory, G. L., Vay, S. A., Brunke, K. E., Kondo, Y., Koike, M., Schlager, H., Baughcum, S. L., Jensen, E., Zhao Y. J., and Kita, K.: An assessment of aircraft as a source of particles to the upper troposphere, *Geophys. Res. Lett.*, 26, 3069–3072, 1999.
- Atkinson, R., Baulch, D. L., Cox, R. A., Hampson, Jr., R. F., Kerr, J. A., Rossi, M. J., and Troe, J.: Summary of evaluated kinetic and photochemical data for atmospheric chemistry: Web Version January 1999, <http://www.iupac-kinetic.ch.cam.ac.uk/index.html>, 01/1999.
- Becker, G., Grooß, J.-U., McKenna, D. S., and Müller, R.: Stratospheric photolysis frequencies: Impact of an improved numerical solution of the radiative transfer equation, *J. Atmos. Chem.*, 37, 217–229, 2000.
- Borrmann, S., Solomon, S., Dye, J. E., and Luo, B. P.: The potential of cirrus clouds for heterogeneous chlorine activation, *Geophys. Res. Lett.*, 23, 2133–2136, 1996.
- Brasseur, G. P., Cox, R. A., Hauglustaine, D., Isaksen, I., Lelieveld, J., Lister, D. H., Sausen, R., Schumann, U., Wahner, A., and Wiesen, P.: European scientific assessment of the atmospheric effects of aircraft emissions, *Atmos. Environ.*, 32, 2327–2422, 1998.
- Carlsaw, K. S., Luo, B. P., and Peter, Th.: An analytic expression for the composition of aqueous  $HNO_3$ - $H_2SO_4$  stratospheric aerosols, *Geophys. Res. Lett.*, 22, 1877–1880, 1995.
- DeMore, W. B., Sander, S. P., Golden, D. M., Hampson, R. F., Kurylo, M. J., Howard, C. J., Ravishankara, A. R., Kolb, E. C.,

- and Molina, M. J.: Chemical kinetics and photochemical data for use in stratospheric modeling, Evaluation Number 12, JPL Publication 97-4, Pasadena, 1997.
- Groß, J.-U.: Modeling of stratospheric chemistry based on HALOE/UARS satellite data results, PhD thesis, Mainz, Shaker Verlag, ISBN 3-8265-1645-1, 1996.
- Hanson, D. R., Ravishankara, A. R., and Solomon, S.: Heterogeneous reactions in sulfuric acid aerosols: A framework for model calculations, *J. Geophys. Res.*, 99, 3615–3629, 1994.
- Hendricks, J., Lippert, E., Petry, H., and Ebel, A.: Heterogeneous reactions on and in sulfate aerosols: Implications for the chemistry of the midlatitude tropopause region, *J. Geophys. Res.*, 104, 5531–5550, 1999.
- Hofmann, D. J., Stone, R. S., Wood, M. E., Deshler, T., and Harris, J. M.: An analysis of 25 years of balloon-borne aerosol data in search of a signature of the subsonic commercial aircraft fleet, *Geophys. Res. Lett.*, 25, 2433–2436, 1998.
- IPCC (Intergovernmental Panel on Climate Change): Aviation and the global atmosphere, (Eds) Penner, J. E., Lister, D. H., Griggs, D. J., Dokken, D. J., and McFarland, M., Cambridge University Press, Cambridge, 1999.
- Kärcher, B.: Heterogeneous chemistry in aircraft wakes: Constraints for uptake coefficients, *J. Geophys. Res.*, 102, 19 119–19 135, 1997.
- Kärcher, B. and Meilinger, S. K.: Perturbation of the aerosol layer by aviation-produced aerosols: A parametrization of plume processes, *Geophys. Res. Lett.*, 25, 4465–4468, 1998.
- Kärcher, B. and Solomon, S.: On the composition and optical extinction of particles in the tropopause region, *J. Geophys. Res.*, 104, 27 441–27 459, 1999.
- Kärcher, B., Turco, R. P., Yu, F., Danilin, M. Y., Weisenstein, D. K., Miake-Lye, R. C., and Busen, R.: A unified model for ultrafine aircraft particle emissions, *J. Geophys. Res.*, 105, 29 379–29 386, 2000.
- Kawa, S. R. (Assessment Chair), Anderson, J. G., Baughcum, S. L., Brock, C. A., Brune, W. H., Cohen, R. C., Kinnison, D. E., Newman, P. A., Rodriguez, J. M., Stolarski, R. S., Waugh, D., and Wofsy, S. C.: Assessment of the effects of high-speed aircraft in the stratosphere: 1998, NASA Technical Paper, TP-1999-209237, June 1999.
- Lary, D. J. and Pyle, J. A.: Diffusive radiation, twilight and photochemistry, *J. Atmos. Chem.*, 13, 373–406, 1991.
- Meilinger, S. K., Kärcher, B., v. Kuhlmann, R., and Peter, Th.: On the Impact of Heterogeneous Chemistry on Ozone in the Tropopause Region, *Geophys. Res. Lett.*, 28, 515–518, 2001.
- Peter, Th., Brühl, C., and Crutzen, P. J.: Increase in the PSC-formation probability caused by high-flying aircraft, *Geophys. Res. Lett.*, 18, 1465–1468, 1991.
- Peter, Th.: Microphysics and heterogeneous chemistry of polar stratospheric clouds, *Annu. Rev. Phys. Chem.*, 48, 785–822, 1997.
- Pitari, G., Mancini, E., Bregman, A., Rogers, H. L., Sundet, J. K., Grewe, V., and Dessens, O.: Sulfate particles from subsonic aviation: Impact on upper tropospheric and lower stratospheric ozone, *Phys. Chem. Earth*, 26, 563–569, 2001.
- Sander, S. P., Friedl, R. R., DeMore, W. B., Golden, D. M., Kurylo, M. J., Hampson, R. F., Huie, R. E., Moortgat, G. K., Ravishankara, A. R., Kolb, E. C., and Molina, M. J.: Chemical kinetics and photochemical data for use in stratospheric modeling, Supplement to Evaluation 12: Update of key reactions, Evaluation Number 13, JPL Publication 00-003, Pasadena, 2000.
- Singh, H. B., Chen, Y., Gregory, G. L., Sachse, G. W., Talbot, R., Blake, D. R., Kondo, Y., Bradshaw, J. D., Heikes, B., and Thornton, D.: Trace chemical measurements from the northern midlatitude lowermost stratosphere in early spring: Distributions, correlations and fate, *Geophys. Res. Lett.*, 24, 127–130, 1997.
- UBA (Umweltbundesamt): Auswirkungen der Emissionen des Luftverkehrs oberhalb der Tropopause auf die stratosphärische Ozonschicht (ALTO), Forschungsbericht No. 29541814 (Luftreinhaltung), Mai 2000.
- Weisenstein, D. K., Ko, M. K. W., Dyominov, I. G., Pitari, G., Ricciardulli, L., Visconti, G., and Bekki, S.: The effects of sulfur emissions from HSCT aircraft: A 2-D model intercomparison, *J. Geophys. Res.*, 103, 1527–1547, 1998.
- WMO (World Meteorological Organisation): Scientific assessment of ozone depletion: 1994, Report No. 37, Geneva, 1994.
- Ziereis, H., Schlager, H., Schulte, P., van Velthoven, P. F. J., and Slemr, F.: Distributions of NO, NO<sub>x</sub> and NO<sub>y</sub> in the upper troposphere and lower stratosphere between 28° and 61° N during POLINAT 2, *J. Geophys. Res.*, 105, 3653–3664, 2000.